

Morphological characterizations of ZnO nanostructures synthesized by hydrothermal method

S. ERTEN-ELA*, S. COGAL, S. ICLI
Solar Energy Institute, Ege University, Bornova, 35100 Izmir, Turkey

An efficient hydrothermal method is presented to synthesize ZnO nanostructures. We investigated the effects of reaction conditions by adjusting the amounts of NaOH, growth temperature, surfactant, annealing to control the morphologies of ZnO nanostructures. Critical amount of NaOH in our reaction system has great influence on the formation of ZnO nanorods. The diameter of ZnO nanocrystals decreased with growth temperature and morphology changed from nanorods to flowers when PEG400 was added to the solution.

(Received March 18, 2009; accepted May 25, 2009)

Keywords: Hydrothermal method, ZnO, Nanorod, Nanoflower, Optical and structural characterization

1. Introduction

ZnO is a promising material for high-performance photonics applications. The properties of ZnO like wide band gap (3.37 eV), high breakdown strength, large excitonic binding energy (60meV), high refractive index, and high recombination efficiency make it a good candidate for use in electro-optic applications like high-efficiency LEDs and LASERs. Other potential applications in the future nano-optoelectronic industry include sensors, luminescent phosphor for displays, photonic crystals, solar cells, field emitter [1,2]. ZnO crystals with different configurations, such as nanorods (nanowires) [3], nanoparticles [4] nanoribbons[5], tetrapods[6], towerlike[7], tubelike [7,8] and flowerlike ZnO [9] have been successfully fabricated. Most techniques to fabricate ZnO nanostructures, such as vapor phase transport deposition [6], chemical vapor deposition [5], pulsed laser ablation [10], electrodeposition [11], ultrasonic irradiation [4], and thermal evaporation [12], are not suitable for controllable synthesis; in addition to being complex processes, sophisticated equipment and economically prohibitive high temperatures are required. Chemical methods, such as sol-gel [7,13], template growth [8,14] and hydrothermal methods [9,15] have been proved to be attractive due to the low growth temperature and easy operation, promising scale-up fabrication.

Solution-phase routes are appealing due to their low growth temperature, low cost, high efficiency, and potential for scaleup. So far, microemulsion, hydrothermal self-assembly and template-assisted sol-gel processes have been employed to synthesize ZnO nanowires and nanorods [16]. ZnO nanostructures as biochemical sensors and as an inorganic dye for labeling cells, taking advantage of their strong visible light emission. On account of these interesting and possibly lucrative applications, ZnO nanostructures are now a widely studied topic [17,18].

ZnO materials have good electrical, optical, and magnetic properties and that the control of the shape and crystal structure is important. It is well known that the addition of impurities into a wide gap semiconductor can often induce dramatic changes in the optical, electrical, and magnetic properties [19-22].

In this paper, we report the synthesis, structural characterization of ZnO nanostructures using a hydrothermal method to prepare different morphologies of nanostructures by adjusting the amount of NaOH, growth temperature, surfactant, annealing. We investigate the NaOH effect on the morphology of ZnO nanostructures. Structural characterization of nanostructures were done by scanning electron microscopy (SEM).

2. Experimental section

2.1 Materials

Sodium hydroxide (NaOH), ethanol absolute (C_2H_5OH), polyethylene glycol (PEG, MW= 400) and zinc acetate dehydrate [$Zn(Ac)_2 \cdot 2H_2O$] were purchased from Aldrich. Solvents were of spectroscopic grade and were used without any further purification.

2.2 Synthesis of ZnO nanostructures

The method used for synthesis of ZnO nanostructures was reported in our previous paper [23]. And schematic diagram of synthesis method is shown in Fig. 1. To investigate the NaOH effects the molar ratio of $ZnAc_2$ and NaOH was changed from 1:1 to 1:8.

For reaction temperature effects we carried out the reaction for three different reaction temperatures (140 °C, 170 °C and 200 °C).

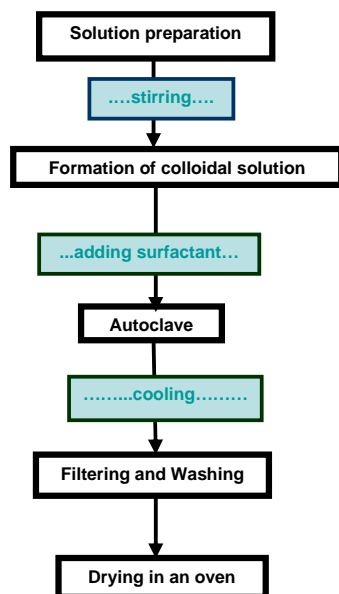


Fig. 1. Schematic diagram of synthesis method.

2.3 Characterization

Scanning electron microscopy (SEM) images were taken with Philips XL-30S FEG scanning electron microscopy. FT-IR measurements were taken Perkin Elmer Spectrum BX FT-IR

3. Results and discussion

3.1 Effects of NaOH on the morphology of ZnO

The molar ratio of ZnAc_2 and NaOH was changed from 1:1 to 1:8 to investigate the influence of NaOH on

the morphology of ZnO. In our study crystalline quality of ZnO nanostructures decrease with the increasing amount of NaOH. To improve the crystalline quality we rinsed the products with diluted HCl to eliminate the impurities (Na^+ and OH^- ions) caused by the excess of NaOH (Fig. 2).

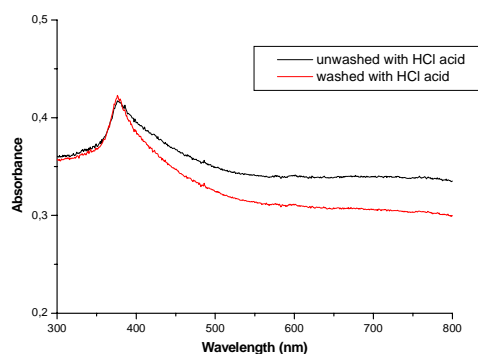


Fig. 2. Effect of washing with HCl acid on the absorption spectrum of ZnO.

Fig. 3 shows the SEM images of ZnO products synthesized with different amount of NaOH. When using different molar ratio of NaOH, all the products were of irregular shapes with a wide size distribution although some of them show nanorod structure (Fig. 3a, b, c). On the other hand, when $\text{Zn}^{2+}/\text{OH}^-$ molar ratio is fixed to 1:8, the products are nanorods with an average diameter of 65 nm and lengths in the range of 300-500 nm (Fig. 3d). From the above results, it is pointed out that 1:8 ratio of $\text{Zn}^{2+}/\text{OH}^-$ is a critical ratio for the formation of ZnO nanorods in our reaction system.

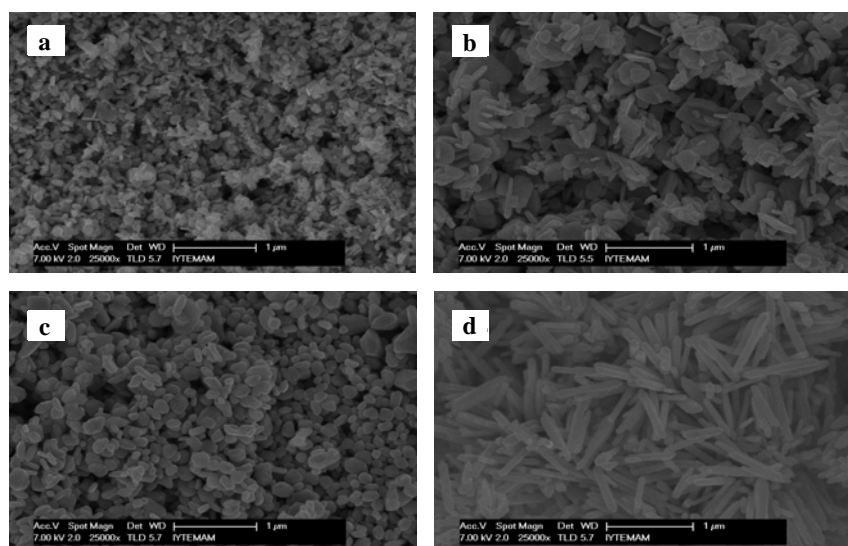


Fig. 3. Effects of NaOH on the morphology synthesized with different molar ratio of Zn^{2+} to OH^- a) 1:1 b) 1:2 c) 1:4 d) 1:8.

3. 2 Effects of PEG400 as a surfactant on the morphology of ZnO

In the aqueous solution, OH^- ions formed due to hydrolysis of the basic additive NaOH and $\text{Zn}(\text{OH})_2$ formed by the reaction between Zn^{2+} and OH^- ions. In dilute solutions, zinc(II) can exist as several monomeric hydroxyl species. These species include $\text{Zn}(\text{OH})^+_{(\text{aq})}$, $\text{Zn}(\text{OH})_{2(\text{aq})}$, $\text{Zn}(\text{OH})_{2(\text{s})}$, $\text{Zn}(\text{OH})_{3^-}^-(\text{aq})$ ve $\text{Zn}(\text{OH})_{4^{2-}}^{2-}(\text{aq})$. The crystal morphology can be controlled by these various species, which act as promoters or inhibitors for nucleation and growth. Solid ZnO nuclei are formed by the dehydration of these hydroxyl species. The ZnO crystal can continue to grow by the condensation of the surface hydroxyl groups with the zinc-hydroxyl complexes [24]. Depending on the amounts of NaOH used, concentration of these species can be changed in the solution. The concentration and kind of each specie cause different growth rate that is responsible for the resulting morphology of the product.

The growth process of ZnO in the presence of PEG400 is different. Because of the existence of surfactant, the surface tension of solution is reduced, which lower the energy needed to form a new phase, and ZnO crystal, therefore, could form in a lower supersaturation [25]. The growth rate, in general, is controlled by external factors like temperature, supersaturation, influence of the solvent, and impurities [26]. In our case, the external factor, i.e. supersaturation caused by the surfactant and the influence of this factor on the nucleation and growth rate of the crystal was studied.

We carried out the same reaction for two different reaction time. PEG400 changes the growth rate of ZnO crystal and the morphology of the final products. Fig. 4 shows the SEM images of ZnO products synthesized in these conditions. The results are in good agreement with the above discussions. From the SEM images it can be clearly observed that in the presence of PEG400 randomly oriented ZnO nanorods were obtained while in the absence of PEG400, ZnO flowers were obtained. As a result, PEG400 as a surfactant plays an important role on the absorption spectra and morphology of ZnO .

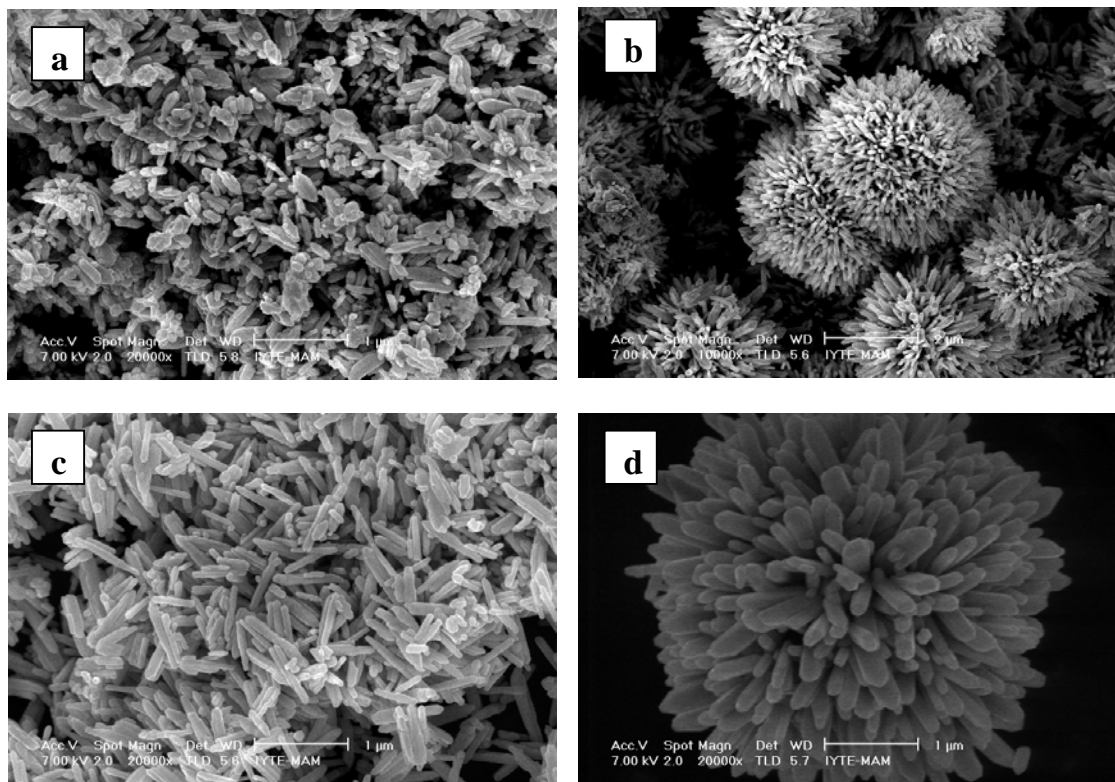


Fig. 4. Effects of PEG400 as a surfactant on the morphology a) ZnO nanorods synthesized at $140\text{ }^\circ\text{C}$ for 6 h in the presence of PEG400 b) ZnO flowers synthesized at $140\text{ }^\circ\text{C}$ for 6 h in the absence of PEG400 c) ZnO nanorods synthesized at $140\text{ }^\circ\text{C}$ for 12 h in the presence of PEG400 d) ZnO flowers synthesized at $140\text{ }^\circ\text{C}$ for 12 h in the absence of PEG400.

3.3 Effects of reaction temperature on the morphology of ZnO

The effect of the reaction temperature on the morphology of the products as also investigated. Fig. 5 shows the SEM images of the products synthesized at different reaction temperature for 6 h. When the reaction proceeded at 140 °C, ZnO nanorods with an average diameter of 50 nm and a length in the range of 300-700 nm were obtained. By increasing the reaction temperature to 170 °C, the ZnO nanorods obtained have an average diameter of 100 nm and length of 250 nm. Upon further increasing the reaction temperature to 200 °C, ZnO nanorods with average diameter of 200 nm and length of 400 nm were detected. As a result, with increasing the reaction temperature average diameter of the ZnO nanorods increases.

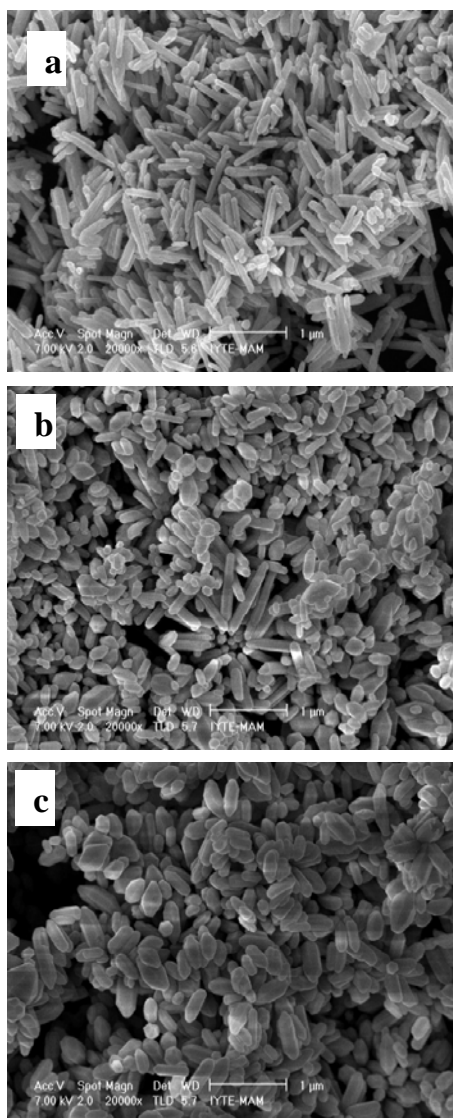


Fig. 5. Effects of reaction temperature on the morphology of ZnO a) 140 °C b) 170 °C c) 200 °C.

3.4 Effects of annealing on the morphology of ZnO

Fig. 6 illustrates the FT-IR spectra of ZnO as prepared and annealed. Note that there is an absorption band corresponding to hydroxyl group (O-H) at 3441 cm^{-1} . The absorption band at $\sim 2400 \text{ cm}^{-1}$ is because of existence of CO_2 molecular in air. The bonds between 500 and 600 cm^{-1} corresponded to the ZnO bonds. After annealing, O-H bonds become weaker indicating decomposition of the organic moieties.

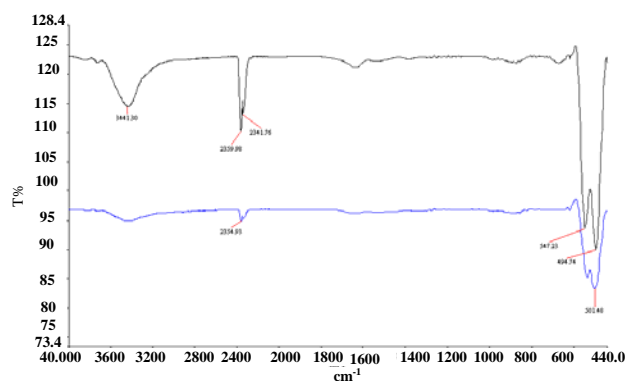


Fig. 6. FT-IR results of ZnO as prepared (black line) and annealed (blue line).

4. Conclusions

We investigated the reaction conditions including NaOH, growth temperature, surfactant and annealing on ZnO products. By using hydrothermal method, ZnO nanostructures with different morphologies were successfully synthesized. The effect of the reaction conditions on the morphological characterization as discussed in detail.

Acknowledgements

We acknowledge financial support from Scientific and Technological Research Council of Turkey, TUBITAK, TBAG_106T061 and the Alexander von Humboldt Foundation of Germany and European Science Foundation (ESF) for research supports. I thank Cagatay ELA for proofreading.

References

- [1] K. Vanheusden, W. L. Warren, C. H. Seager, D. R. Tallant, J. A. Voigt, B. E. Gnade, *J. Appl. Phys.* **79**, 7983 (1996).
- [2] J. W. P. Hsu, D. R. Tallant, R. L. Simpson, N. A. Missert, R. G. Copeland, *Appl. Phys. Lett.* **88**,

- 252103 (2006).
- [3] B. Cheng, E. T. Samulski, *Chem. Commun.* **986**, (2004).
- [4] D. Qian, J. Z. Jiang, P. L. Hansen, *Chem. Commun.* 1078 (2003).
- [5] P. M. Gao, Y. Ding, W. J. Mai, W. L. Hughes, C. S. Lao, Z. L. Wang, *Science* **309**, 1700 (2005).
- [6] P. Yang, H. Q. Yan, S. Mao, R. Russo, J. Johnson, R. Saykally, N. Morris, J. Pham, R. He, H. J. Choi, *Adv. Funct. Mater.* **12**, 323 (2002).
- [7] Z. Wang, X. F. Qian, J. Yin, Z. K. Zhu, *Langmuir* **20**, 3441 (2004).
- [8] X. P. Shen, A. H. Yuan, Y. M. Hu, Y. Jiang, Z. Xu, Z. Hu, *Nanotechnology* **16**, 2039 (2005).
- [9] H. Zhang, D. R. Yang, Y. J. Ji, X. Y. Ma, J. Xu, D. L. Que, *J. Phys. Chem. B* **108**, 3955 (2004).
- [10] Y. Sun, G. M. Fuge, M. N. R. Ashfold, *Chem. Phys. Lett.* **396**, 21 (2004).
- [11] B. Q. Cao, W. P. Cai, G. T. Duan, Y. Li, Q. Zhao, D. P. Yu, *Nanotechnology* **16**, 2567 (2005).
- [12] Z. W. Pan, Z. R. Dai, Z. L. Wang, *Science* **291**, 1947 (2001).
- [13] K. F. Lin, H. M. Cheng, H. C. Hsu, L. J. Lin, W. F. Hsieh, *Chem. Phys. Lett.* **409**, 208 (2005).
- [14] X. H. Zhang, S. Y. Xie, Z. Y. Zhang, Z. Q. Tian, Z. X. Xie, R. B. Huang, L. S. Zheng, *J. Phys. Chem. B* **107**, 10114 (2003).
- [15] J. P. Cheng, X. B. Zhang, X. Y. Tao, H. M. Lu, Z. Q. Luo, F. Liu, *J. Phys. Chem. B* **110**, 10348 (2006).
- [16] B. Wen, Y. Huang, J. J. Boland, *J. Phys. Chem. C* **112**, 106 (2008).
- [17] T. Kawano, H. Imai, *Cryst. Growth Des.* **6**, 1054 (2006).
- [18] B. Reeja-Jayan, E. De la Rosa, S. Sepulveda-Guzman, R. A. Rodriguez, M. J. Yacaman *J. Phys. Chem. C* **112**, 240 (2008).
- [19] P. Yang, H. Yan, S. Mao, R. Russo, J. Johnson, R. Saykally, N. Morris, J. Pham, R. He, H. J. Choi, *Adv. Funct. Mater.* **12**, 319 (2002).
- [20] B. B. Lia, X. Q. Xiua, R. Zhanga, Z. K. Taoa, L. Chena, Z. L. Xie, Y. D. Zheng, *Mater. Sci. Semicond. Proc.* **9**, 141 (2006).
- [21] G. Sanon, R. Rup, A. Mansingh, *A. Phys. Rev. B* **44**, 5672 (1991).
- [22] D. Wu, M. Yang, Z. Huang, G. Yin, X. Liao, Y. Kang, X. Chen, H. Wang, *J. of Colloid and Interface Science* **330**, 380 (2009).
- [23] S. Erten-Ela, S. Cogal, S. Icli, *Inorganica Chimica Acta*, in print, 2008, doi:10.1016/j.ica.2008.08.038
- [24] L. E. Greene, B. D. Yuhas, D. Zitoun, P. Yang, *Inorganic Chemistry* **45**, 7535 (2006).
- [25] X. M. Sun, X. Chen, Z. X. Deng, Y. D. Li, *Materials Chemistry and Physics* **78**, 99 (2002).
- [26] M. Bitenc, Z. C. Orel, *Materials Research Bulletin* **44**, 381 (2009).

*Corresponding author: suleerten@yahoo.com
sule.erten@ege.edu.tr